

## COMPOSITION OPTIMIZATION OF TWO DIMENSIONAL FUNCTIONALLY GRADED MATERIALS UNDER THERMAL LOADING

---

**Mahmoud Nemat-Alla**

Mechanical Engineering Department, Faculty of Engineering, Assiut University, Assiut71516, Egypt

(Received November 2, 2008 Accepted November 18, 2008)

*Reduction of the thermal stresses in machine elements that are subjected to severe thermal loadings was achieved by developing two-dimensional functionally graded material, 2D-FGM. In the current investigation composition optimization for  $ZrO_2/6061-T6/Ti-6Al-4V$  2D-FGM, under severe thermal loading cycle that consists of heating followed by cooling, was carried out based on the minimization of temperatures, thermal and residual stresses to achieve more reduction of the thermal stresses. It was found that optimum composition based on minimum value of the maximum temperature for  $ZrO_2/6061-T6/Ti-6Al-4V$  2D-FGM was achieved for  $m_x = 0.1$  and  $m_y = 0.1$ . While optimum composition based on minimum value of the maximum normalized equivalent stresses for  $ZrO_2/6061-T6/Ti-6Al-4V$  2D-FGM was achieved for  $m_x = 0.1$  and  $m_y = 5$ , where  $m_x$  and  $m_y$  are the composition variation parameters in  $x$  and  $y$  directions respectively. Also, the obtained optimum composition of  $ZrO_2/6061-T6/Ti-6Al-4V$  2D-FGM can stand well with the adopted severe thermal loading without any plastic deformation or residual stresses where the maximum value of the normalized equivalent stresses during heating stage was 0.8 and the maximum value of the normalized equivalent stresses during cooling stage was 0.24.*

**KEYWORDS:** *Composition optimization, 2D-FGM, Nonhomogenous parameters, Elastic-plastic material model, Temperature dependent material properties, Thermal stresses, Finite element analysis.*

### 1. INTRODUCTION

Functionally graded materials (FGMs), whose compositional gradients are designed to have unique properties, that are not available from a homogenous material, have great potential for thermal barrier applications [1-5]. FGMs overcome the drawbacks of the multi-layers composite plates that have been commonly used as thermal barrier [6,7], such as cracking.

The temperature distributions in machine elements that are used in several applications such as space shuttles, nuclear reactors, aircrafts, ovens, combustion chambers, etc, change in two or three directions. For example, Steinberg [8] showed that the temperature distribution on the outer surface of new aerospace craft, when the plane is in sustained flight at a speed of Mach 8 and altitude of 29 km, the temperature

on the outer surface of such a plane ranges from 1033 K along the top of the fuselage to 2066 K degrees at the nose. Furthermore, this temperature level has to decay severely, through the thickness of the craft body, to the room temperature inside the craft. Such kind of aerospace craft added a new challenge to introduce and develop more effective high-temperature resistant materials that can withstand high-external temperatures that have variations in two or three directions. Thus, proper and efficient operation of such machine elements necessitates the use of effective high-temperature resistant materials. To overcome such problem Callister [9] suggested the use of several different thermal protection materials, which satisfy the required criteria, for a specific region of the space craft surface. However, this design has the same drawbacks of the composite layers which were overcome by using FGM [6].

In 2003, the Colombia space shuttle was lost in a catastrophic break up due to outer surface insulation that fell loose when the Columbia lifted off. The physical cause of the loss of Columbia and its crew was a breach in the thermal protection system on the leading edge of the left wing, caused by a piece of insulating foam which separated from the left bipod ramp section of the external tank and struck the wing in the vicinity of the lower half of reinforced carbon-carbon panel. During re-entry this breach in the thermal protection system allowed superheated air to penetrate through the leading edge insulation and progressively melt the aluminum structure of the left wing, resulting in a weakening of the structure until increasing aerodynamic forces caused loss of control, failure of the wing, and break-up of the Orbiter [10, 11]. Such damage to the space shuttle's protective thermal tiles can be prevented by using FGMs. It is worth mentioning that conventional FGM may also not be so effective in the design of such advanced machine elements. This adds a new challenge to introduce and develop more effective high-temperature resistant materials that can stand with such applications. Therefore, *two-dimensional functionally graded materials* (2D-FGMs) that have two-dimensional properties, which may have more effective high-temperature resistant, were introduced.

Many investigations [12-19] for 2D-FGMs have been carried out. Unfortunately, all of them have considered exponential functions for continuous gradation of the material properties. The use of exponential functions for the variation of the material properties usually facilitates the analytical solution but don't give real representation for the material properties, except for the upper and lower surfaces of FGM. Aboudi *et al.* [20, 21] studied response of laminated plates subjected to temperature change in one dimension. They found that it is possible to reduce the magnitude of thermal stress concentrations by a proper management of the microstructure of the composite.

Cho *et al.* [22] have optimized the volume fractions distributions of FGM for relaxing the effective thermal stresses. They obtained the optimal volume fractions distribution in two directions. The obtained optimum volume fractions have a random and not practical distribution, which can not represent or simulate FGM that have continuous variations of the composition. Goupee and. Vel [23] proposed a methodology for the two-dimensional simulation and optimization of material composition distribution of FGM. Two-dimensional quasi-static heat conduction problem was analyzed using the element-free Galerkin method. They obtained spatial

distribution of volume fractions by piecewise bi-cubic interpolation. The obtained optimum volume fractions have also a random distribution.

The concept of adding a third material constituent to the conventional FGM to withstand the induced severe thermal stresses was introduced by Nemat-Alla [24]. The introduced model of 2D-FGM has continuous composition variations in two directions. It has three basic constituent materials, at least one of them is ceramic material while the remainder are metallic materials. The rules of mixture and the volume fractions relations were introduced. Comparison between the 2D-FGM and conventional FGM was carried out and showed that 2D-FGM has high capability in reducing thermal stresses than conventional FGM. It is worth mentioning that temperature independent properties and elastic behavior of the FGMs have been considered through most of the above mentioned investigations. Therefore, realistic investigations of 2D-FGMs should be carried out considering the temperature dependent properties and elastic-plastic behavior of the 2D-FGMs.

Recently, a new method for manufacturing of FGMs via inkjet color printing has been reported by Wang and Shaw [25]. According to this method  $\text{Al}_2\text{O}_3$  and  $\text{ZrO}_2$  aqueous suspensions were stabilized electrostatically and placed in different color reservoirs in inkjet cartridges. The volume and composition of the suspensions printed in droplets at a small area were controlled by the inkjet cyan–magenta–yellow– black color printing principle. The proposed method shows the potential for the manufacturing of FGMs with arbitrarily 2D and 3D composition profiles. Therefore it can be properly applied to manufacture the 2D-FGM model proposed by Nemat-Alla [24]. Nemat-Alla *et al.* [26] investigated the capability of 2D-FGM in standing with two-dimensional severe thermal loads over the conventional FGM. Temperature dependent material properties and elastic-plastic behavior of the 2D-FGM were considered. Four alternatives of FGMs are adopted namely;  $\text{ZrO}_2/\text{Ti-6Al-4V}$  conventional FGM,  $\text{ZrO}_2/6061\text{-T6}$  conventional FGM,  $\text{ZrO}_2/\text{Ti-6Al-4V}/6061\text{-T6}$  2D-FGM and  $\text{ZrO}_2/6061\text{-T6}/\text{Ti-6Al-4V}$  2D-FGM. Elastic-plastic stress analysis of the considered plates under the same transient thermal loading cycle was carried out. It was found that only  $\text{ZrO}_2/6061\text{-T6}/\text{Ti-6Al-4V}$  2D-FGM can withstand the adopted thermal loading without fracture. It is worth noting that a single case of the composition variations in x-direction, linear variation, was adopted by Nemat-Alla *et al.* [26].

In the current investigation it is planned to achieve more reduction of thermal stresses under two-dimensional severe thermal loading adopting the optimum case that obtained by Nemat-Alla *et al.* [26] which was  $\text{ZrO}_2/6061\text{-T6}/\text{Ti-6Al-4V}$  2D-FGM, that only could stand with severe two-dimensional thermal loading. This can be achieved by the composition optimization of the adopted  $\text{ZrO}_2/6061\text{-T6}/\text{Ti-6Al-4V}$  2D-FGM. Composition optimization will be carried out through the variations of the compositions in x and y-directions by changing the values of the nonhomogenous parameters in x- and y-directions.

## 2. FUNCTIONALLY GRADED MATERIAL MODELING

### 2.1. Volume Fractions of 2D-FGM

The adopted  $ZrO_2/6061-T6/Ti-6Al-4V$  2D-FGM is made of continuous gradation of three distinct materials [24]. The composition changes from  $ZrO_2$  at the upper surface to 6061-T6 alloy at the lower left corner and Ti-6Al-4V at the lower right corner. The basic constituents of the adopted 2D-FGM plate are varied continuously in a predetermined composition profile according to the volume fractions distributions that are controlled by the nonhomogenous parameters  $m_x$  and  $m_y$  in  $x$  and  $y$ -directions respectively. Therefore, nonhomogenous thermal and mechanical properties of the adopted 2D-FGM plate which are varied in both of thickness and width directions are considered.

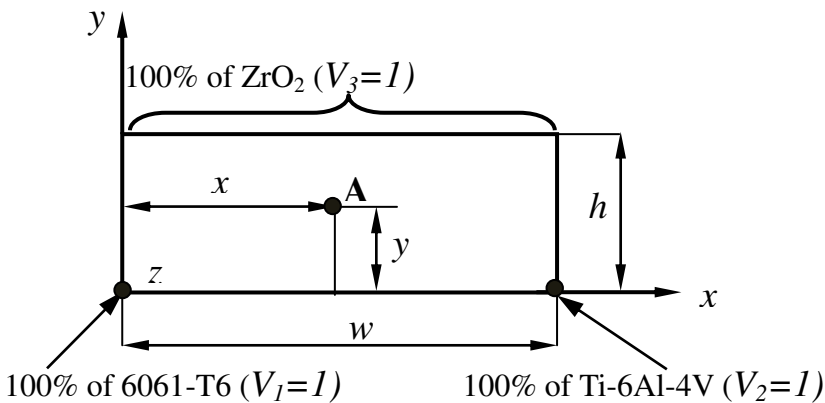


Fig. 1. Dimensions and coordinate system of the considered  $ZrO_2/6061-T6/Ti-6Al-4V$  2D-FGM plate.

The dimensions of the considered plate are; 30 mm thickness  $h$ , 300 mm width  $w$  and 700 mm length as shown in Fig. 1. Through the current investigation  $x$ ,  $y$  and  $z$  coordinates coincide with the directions of the width, thickness and length of the FGM plates respectively.

The volume fractions of the 2D-FGM plate at an arbitrary location (point A) are expressed as [24];

$$V_1 = \left[ 1 - \left( \frac{y}{h} \right)^{m_y} \right] \left[ 1 - \left( \frac{x}{w} \right)^{m_x} \right] \quad (1)$$

$$V_2 = \left[ 1 - \left( \frac{y}{h} \right)^{m_y} \right] \left( \frac{x}{w} \right)^{m_x} \quad (2)$$

$$V_3 = \left( \frac{y}{h} \right)^{m_y} \quad (3)$$

Where  $V_1$ ,  $V_2$  and  $V_3$  represent the volume fractions of 6061-T6, Ti-6Al-4V and  $ZrO_2$  respectively.  $m_x$  and  $m_y$  are the nonhomogenous parameters that represent the

composition variations in  $x$  and  $y$  directions respectively. The composition of the 2D-FGM adopted in the present analysis changes through the thickness  $h$  from 100 %  $ZrO_2$  at the upper surface,  $y = h$ , to a FGM of two different metals on the lower surface,  $y = 0$ . The FGM of two different metals at the lower surface of the plate also changes from 100% 6061-T6 aluminum alloy at left corner,  $x = 0$  and  $y = 0$ , to 100% Ti-6Al-4V at the right corner,  $x = w$  and  $y = 0$ .

The porosity of the 2D-FGM is defined as;

$$p = A_y \left(\frac{y}{h}\right)^{m_y} (p_y - p_x) + p_x \quad (4)$$

where  $A_y$ ,  $p_x$  and  $p_y$  are known functions [24].

## 2.2. Rules of Mixtures and Temperature Dependent Material Properties

The rules of mixtures for the 2D-FGM introduced by Nemat-Alla [24] were adopted through the current investigations. They were used to calculate the variations of the material properties for the 2D-FGM plate at different values of the nonhomogenous parameters  $m_x$  and  $m_y$ . Also, the thermo-mechanical properties of  $ZrO_2$ , 6061-T6 aluminum alloy and Ti-6Al-4V in [4, 5, 27, 28] were adopted during the current investigations. It is noteworthy that the variations of the thermo-mechanical properties of 6061-T6 aluminum alloy versus temperatures are represented graphically in [5] and curve fitting approximations were carried out to express them in the formulae forms. Also, the yield stress,  $\sigma_y$ , stiffness coefficient,  $k$ , and strain hardening exponent,  $n$ , of 6061-T6 aluminum alloy and Ti-6Al-4V versus temperatures are represented graphically in [27] and curve fitting approximations were carried out to obtain them in formulae forms too.

## 2.3. Elastic-Plastic Material Model

The two mathematical material models; bi-linear and power law strain hardening are commonly used to represent the elastic-plastic behaviors of most of engineering materials. Previous studies [20, 21, 29-36] have adopted the bilinear hardening models for ceramic/metal FGMs to evaluate the material properties (yield stress and tangent modulus) using the volume fractions and rules of mixtures. The power law strain hardening model has been recently adopted in some studies, [37-40], for ceramic/metal conventional FGMs to evaluate the material properties using the volume fractions and rules of mixtures. All the above investigations were carried out for conventional FGM. Of course power law strain hardening model is more realistic in representing the material behavior than bilinear hardening model. The elastic-plastic models mentioned above can be applied for conventional FGM only. In order to use such elastic-plastic models for 2D-FGM it needs some mathematical treatments which are not available now. Nemat-Alla et al. [26] introduce power law strain hardening model for 2D-FGM which will be adopted in the current investigations of  $ZrO_2/6061-T6/Ti-6Al-4V$  2D-FGM. It is noteworthy that for the ceramic constituent material,  $ZrO_2$ , the values of the yield strength are assigned by the values of the ultimate strength. Also, for applying power law strain hardening model on  $ZrO_2$  the strain hardening exponent value was

unity and the strength coefficient values were equal to the elastic modulus values. This represents the elastic behavior of  $ZrO_2$  when using power law hardening model.

### 3. $ZrO_2/6061-T6/Ti-6Al-4V$ 2D-FGM COMPOSITION OPTIMIZATION

In the course of the current investigation a finite element model was developed in conjunction with an optimization algorithm to obtain an optimal compositional distribution for  $ZrO_2/6061-T6/Ti-6Al-4V$  2D-FGM plate. Composition optimization process aims at obtaining the optimal compositions for  $ZrO_2/6061-T6/Ti-6Al-4V$  2D-FGM plate that is subjected to the given design variables and objectives. The optimization processes identify the distribution of the material composition within the design domain to minimize the thermal and residual stresses. In order to deal with the composition optimization of the 2D-FGM, to minimize the thermal and residual stresses, a normalized stress that represents a critical value should be adopted. Therefore, in order to represent the thermal stresses in an indicative manner it should be normalized by the yield strength or tensile strength. Composition optimization for non-homogenous cylinder under thermal load adopting elastic analysis was carried out by Tanigawa et al. [27]. They used the tensile strength in the normalizing process as an indicative parameter for failure process. Since FGM is usually used in applications that must have high reliability and safety, such as space shuttles and nuclear reactors, therefore, normalizing process of thermal stresses by the yield strength is better in such applications to insure their high reliability and safety. According to this discussion the yield strength will be adopted in the normalized processes during the current investigation.

The main objective of the current investigation is to minimize the thermal and residual stresses where the normalized von Mises equivalent stress ratio was adopted to indicate them. The yield stresses for the 2D-FGM that used in the normalized stresses were calculated at the different positions according to the rule of mixture of 2D-FGM. It is noteworthy that the tensile yield stresses for the  $ZrO_2$  constituent are considered if the first principle thermal stress component is tension. While compressive yield stresses are considered when the first principle thermal stress component is compression.

The design variables for this problem are the nonhomogenous parameter  $m_x$  and  $m_y$  that controls the composition variations through the 2D-FGM plate and hence the variations of thermal and mechanical properties of the 2D-FGM in x- and y-directions. The following conditions for the design variables are considered;

- The values of the nonhomogeneous parameter,  $m_x$ , are varying in the range  $0 \leq m_x \leq \infty$ . Zero value is represented by 0.1 to obtain a 2D-FGM and  $\infty$  is represented by 20. Where  $m_x = 0.1$ , 2D-FGM, is better than  $m_x = 0.0$ , conventional FGM, in reduction of thermal stresses according to Nemat-Alla et al. [26]. Also,  $m_x = \infty$  is represented by 20 where higher values have negligible effect in the variations of the composition according to Noda [7]. Also,  $m_x = \infty$  represent  $ZrO_2/ Ti-6Al-4V$  conventional FGM. It is worth mentioning that for  $m_x < 1$  the composition is Ti-6Al-4V alloy rich. For  $m_x > 1$  the composition is 6061-T6 alloy rich.

- The values of the nonhomogeneous parameter,  $m_y$ , are varying in the range  $0 \leq m_y \leq \infty$ . Zero value is represented by 0.1, where real zero value represents a ceramic,  $ZrO_2$ , plate. Also,  $m_y < 0.1$  means that the whole of the plate will be brittle like  $ZrO_2$ . It is worth mentioning that for  $m_y < 1$  the composition is 6061-T6/Ti-6Al-4V FGM alloys rich. Also,  $m_y = \infty$  is represented by 20 according to Noda [7]. Where  $m_y = \infty$  represents  $ZrO_2/6061-T6/Ti-6Al-4V$  2D-FGM rich of  $ZrO_2$ .
- Heating time,  $t$ , is varying from zero second to the time required to reach steady state temperatures.
- Cooling time,  $t$ , is starting from the time required for the heating steady state temperatures that represents the time at the end of heating, to the time required for the whole plate to reach a temperature 300 K.

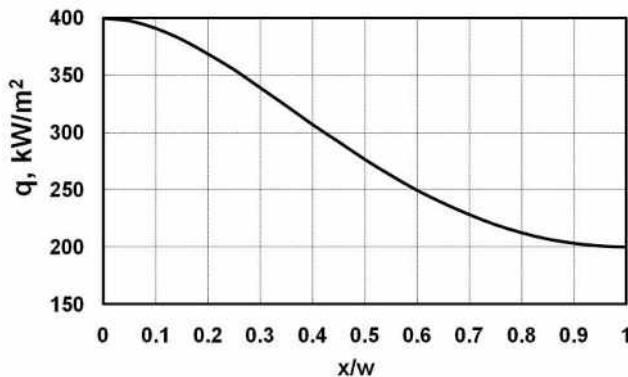


Fig. 2. Non-uniform heat flux that applied on the upper surface of the  $ZrO_2/6061-T6/Ti-6Al-4V$  2D-FGM plate.

#### 4. TRANSIENT THERMAL LOADING

Nemat-Alla *et al.* [26] investigated the effectiveness of  $ZrO_2/6061-T6/Ti-6Al-4V$  2D-FGM in reducing the thermal stresses under severe thermal loading cycle. The thermal loading cycle consists of heating under severe variable heat flux then cooling to room temperature. Such thermal load represents the severe practical applications that many machine elements are subjected to it. Nemat-Alla *et al.* [26] found that conventional and 2D FGM were yielded and have equivalent thermal stress values greater than the tensile strength except the case of  $ZrO_2/6061-T6/Ti-6Al-4V$  2D-FGM. In case of  $ZrO_2/6061-T6/Ti-6Al-4V$  2D-FGM maximum value of normalized equivalent stresses was 1.1 in heating stage and 1.0 in cooling stage. Therefore, the same severe thermal loading cycle that was used by Nemat-Alla *et al.* [26] will be adopted through the current composition optimization process, for  $ZrO_2/6061-T6/Ti-6Al-4V$  2D-FGM.

The thermal loading cycle and the associated boundary conditions are described as follows; firstly, the plate is assumed to be subjected to a nonuniform heating heat flux on the upper surface ( $y = h$ ) as shown in Fig. 2. The applied nonuniform heat flux has the following form:

$$q = (q_{max} - q_{min}) \sin \left[ \left( \frac{\pi}{2} \right) * \left( 1 - \frac{x}{w} \right)^m \right] + q_{min} \tag{5}$$

where  $q_{\max}$  and  $q_{\min}$  are the maximum and minimum values of the heat flux and  $m$  is a constant. Values of  $q_{\max}$  and  $q_{\min}$  were taken to be  $400 \text{ kW/m}^2$  and  $200 \text{ kW/m}^2$ , [6, 41].

The lower surface of the plate, ( $y = 0$ ), is subjected to cooling by convection to an ambient temperature of  $300 \text{ K}$ . The right and left surfaces of the plate, ( $x = 0$ ,  $x = w$ ), are thermally isolated. According to Choules and Kokini [6] and Kokini and Case [41] a convection heat transfer coefficient  $h_L = 1000 \text{ W/m}^2\text{K}$  and  $300 \text{ K}$  ambient temperature are adopted.

After the heating stage reached had to the steady state condition the upper surface was left to cool down by convection to the ambient temperature of  $300 \text{ K}$ . The cooling heat transfer coefficient at the upper surface,  $h_{Uc}$  is taken to be  $1000 \text{ W/m}^2\text{K}$  according to Kokini and Case [41].

The transient temperature,  $T(x, y, \tau)$ , variation over the plate in  $x$  and  $y$  directions is determined by solving the following transient two dimensional heat equation using finite element method:

$$\frac{\partial \lambda}{\partial x} \frac{\partial T(x, y, \tau)}{\partial x} + \frac{\partial \lambda}{\partial y} \frac{\partial T(x, y, \tau)}{\partial y} + \lambda \left( \frac{\partial^2 T(x, y, \tau)}{\partial x^2} + \frac{\partial^2 T(x, y, \tau)}{\partial y^2} \right) = \rho c \frac{\partial T(x, y, \tau)}{\partial \tau} \quad (6)$$

The corresponding thermal boundary conditions for heating and cooling stages are as follows:

Initial condition

$$T(x, y, 0) = 300K \quad (7)$$

Heating stage at the top surface

$$-\lambda \frac{\partial T(x, y, \tau)}{\partial y} \Big|_{y=h} = q \quad (8)$$

Heating and cooling stages at the lower surface

$$\lambda \frac{\partial T(x, y, \tau)}{\partial y} \Big|_{y=0} = h_L [T(x, 0, \tau) - 300] \quad (9)$$

Cooling stage at the top surface

$$\lambda \frac{\partial T(x, y, \tau)}{\partial y} \Big|_{y=h} = h_{Uc} [T(x, 0, \tau) - 300] \quad (10)$$

The isolated thermal boundary conditions at the right and left plate surfaces are as follows;

$$\lambda \frac{\partial T(x, y, \tau)}{\partial x} \Big|_{x=0} = 0 \quad (11)$$

$$\lambda \frac{\partial T(x, y, \tau)}{\partial x} \Big|_{x=w} = 0 \quad (12)$$

## 5. FINITE ELEMENT MODEL

Significant efforts [42-48] have been done in previous researches to implement the continuous variation of the FGM properties in the finite element formulations. It was found that the continual spatial variation of the properties of nonhomogenous materials in the finite element formulation does not present a computational problem

since the stiffness matrix may be determined by averaging across each element. Generally there are two methods that can be adopted to account for the material properties in the finite element formulation. Either through assignment of the properties for each element individually or dividing the whole structure into numerous areas then assigning properties to each area [43-45]. Santare and Lambros [46] introduced a formulation for calculation of material properties in graded elements which automatically interpolates the material properties within the element. Also, Li et al. [42] and Kim and Paulino [47] have proposed a generalized isoparametric formulation in their application of the finite element for materials with an internal property gradient. In these studies, mean properties, calculated by integration within each element, were used for the stiffness matrix. Rousseau and Tippur [48] have introduced a novel technique that involves definition of the properties as functions of the temperature then the properties have been estimated from the solution of these functions after assignment of temperature values at the elements nodes.

In the current investigations temperature dependent thermo-mechanical properties are taken into consideration through the finite element analysis. In order to obtain more accurate predictions of thermal stresses that are expected to be induced in the adopted FGM plates the thermo-elastic-plastic behavior of the constituent materials should be considered. When the upper ceramic surface of FGM plate is subjected to thermal cyclic load (heating followed by cooling) thermal stresses will develop inside the plate. This is attributed to the difference in the coefficient of thermal expansion from point to point inside the plate where the thermal and mechanical properties vary continuously in  $x$  and  $y$  directions. The thermo-mechanical properties are calculated based on volume fractions and the rules of mixture of FGM as described in [24].

Although the material properties of the 2D-FGM plate and the thermal loadings change only in the  $x$ - $y$  plane the thermal strains would create 3D stress strain fields. For assessing the 2D approximation for such case, an aluminum plate similar to that of the 2D-FGM plate was modeled with 3D, 2D plane strain, and 2D plane stress FE models [49]. These models were loaded with a varying temperature field in  $x$ - $y$  plane similar to the adopted field on the current study. The results show that the deviations were about 39% in  $\sigma_y$  for plane strain approximation and 29% in  $\sigma_x$  for plane stress approximation. While the other stress components are closed to their corresponding components of 3D model. Such results prove the essentiality of the using of the 3D model. Since there is no temperature gradient in  $Z$  direction therefore there is neither stress nor strain gradients in  $Z$  direction. However, due to the temperature changes in  $X$ - $Y$  plane, the stresses and strains in  $Z$  directions are not zeros. Then the problem is neither plane stress nor plane strain problem. Furthermore, the problem has 3D Stress-Strain state. Any other assumption may leads to none real stresses or strains in  $Z$  direction. Adding, the problem then has to be analyzed in 3D FE-analysis, while the results of the gradients will be presented in 2D ( $X$ - $Y$ ) contours. The investigated FGM plates have a thickness  $h$  of 30 mm, a width  $w$  of 300 mm and a length of 700 mm. The 3D finite element model, used in the current computations of the coupled elastic-plastic thermo-mechanical problem, contains 46080 eight-nodded thermal-solid brick elements. This number of elements results from uniform dividing

of the FGM into 240 elements through plate width, 24 elements through plate thickness and 8 elements through plate length. The mesh is refined in the plate cross section, x-y plane, (240x 24 elements) because of the material nonhomogeneity in this plane. Such refinement is expected to guarantee more accuracy of the results. On the other hand, a small number of elements (8 elements) have been taken along the plate length, because of the material homogeneity along that direction. Since, there is neither stress nor strain gradients in the Z direction, then there is no harm of using large aspect ratio in this direction.

The mechanical boundary conditions used in the finite element model are as follows; all nodes at the plate bottom surface are roller supported to prevent their movement in the y-direction. Also nodes at the plate left side surface ( $x = 0$ ) and the plate mid plane ( $z = 0$ ) are prevented from movement in the x and z- direction respectively.

The numerical solutions of the present investigation have been carried out for  $ZrO_2/6061-T6/Ti-6Al-4V$  2D-FGM plates of different composition according to the following steps:

- 1- The plate is numerically subjected to a non-uniform heating from the surrounding medium followed by sudden cooling.
- 2- The transient temperature distribution is obtained at discrete time increments by the solution of the thermal problem equations (6-12).
- 3- The resulting displacements and thermal stresses were determined by the solution of the 2D-FGM thermal stresses problem under the predetermined temperature distribution as described above.
- 4- The stresses on each node were averaged according to the stresses on its associated elements and shape function.

Assuming that the plate deformations did not affect the temperatures where, the problem was modeled as a quasi-static thermo-mechanical problem.

## 6- RESULTS AND DISCUSSIONS

Nemat-Alla *et al.* [26] showed that  $ZrO_2/6061-T6/Ti-6Al-4V$  2D-FGM plate has high capability to stand with the adopted thermal load without cracking or fracture. The current work is aimed at getting more reduction of the thermal stresses in  $ZrO_2/6061-T6/Ti-6Al-4V$  2D-FGM plate by composition optimization as described above. The nodal temperatures were obtained by solving the transient heat transfer problem. Elastic-plastic transient structural analysis model of the considered plates, using the obtained temperatures, was used to determine the resulting stresses and displacements under the adopted transient thermal loading cycle. The calculated values of the thermal stresses are normalized by their correspondence yield stresses. The yield stresses are calculated at different positions as a function of the corresponding temperatures at those positions. Through the current investigations it is considered that cracks initiations and propagations will occur when the normalized equivalent stresses are tensile and greater than unity. Since von Mises equivalent stress criteria could not distinguish between compressive and tensile stresses, the first principle stresses will be used to indicate that the equivalent stresses are compressive or tensile. In order to optimize the composition of the adopted 2D-FGM plates based on minimum values of

thermal stresses the parameters that affect the thermal stresses should be investigated. Of course the temperature variation through the adopted 2D-FGM plates is an important parameter, which reflects the effect of thermal conductivity, heat capacity and density.

### 6-1- Reduction of Temperature

In this section the temperatures variation through the adopted  $ZrO_2/6061-T6/Ti-6Al-4V$  2D-FGM plates are presented and discussed. The composition variations of the adopted 2D-FGM plates are represented by the variation of the non homogenous parameters  $m_x$  and  $m_y$  in the x and y directions. Many cases of  $ZrO_2/6061-T6/Ti-6Al-4V$  2D-FGM plates are investigated and the maximum value of the temperature through the plate was assigned. Figure 3 shows the variations of the maximum temperature, in Kelvin, versus the values of the nonhomogenous parameters  $m_x$  and  $m_y$ . It is clear that maximum temperature, 2200 K, occurred at the minimum values of  $m_x$  and  $m_y$ . Minimum values of  $m_x$  and  $m_y$  according to equations (1) to (3) means that the plate is  $ZrO_2$  extremely rich or whole of the plate is  $ZrO_2$ . This case of material composition should be avoided due to low fracture toughness and low strength of  $ZrO_2$ . Also it is clear that the minimum temperatures were achieved for values of  $m_x$  and  $m_y$  which are greater than 6. Maximum values of  $m_x$  and  $m_y$  according to equations (1) to (3) means that the plate is aluminum alloy, 6061-T6, rich. This may be attributed to the fact that aluminum alloy, 6061-T6, has high heat conductivity.

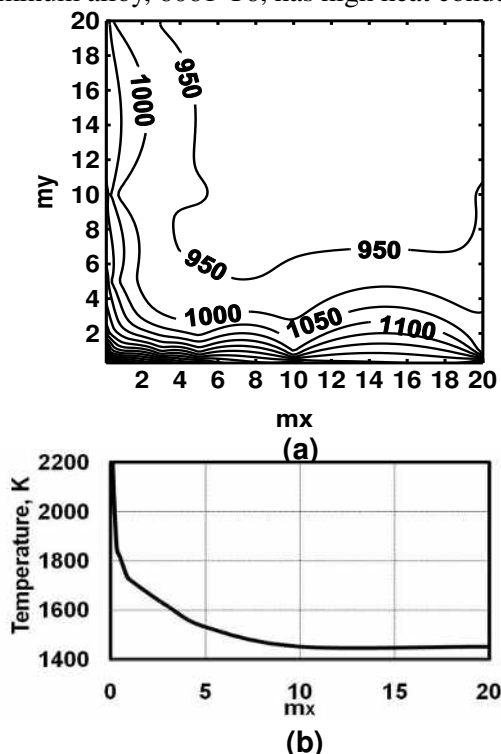


Fig. 3 Variation of maximum temperatures, in Kelvin, for the adopted  $ZrO_2/6061-T6/Ti-6Al-4V$  2D-FGM plates where the maximum value is 2200 K. (a) For different values of  $m_x$  and  $m_y$ . (b) For different values of  $m_x$  and  $m_y = 0$ .

Figure 4 shows the temperature variations, in Kelvin, through  $ZrO_2/6061-T6/Ti-6Al-4V$  2D-FGM plate for  $m_x=0.1$  and  $m_y=0.1$  where the maximum value is 2200 K. The nonhomogenous parameters,  $m_x=0.1$  and  $m_y=0.1$ , represent the case of 2D-FGM plate with ceramic,  $ZrO_2$ , extremely rich. Such case represents the worst case of temperature since maximum temperature was achieved. It is noticeable that the maximum temperature was achieved on the upper ceramic surface which has low fracture toughness and low strength. Therefore such case should be avoided because of achieving maximum temperature.

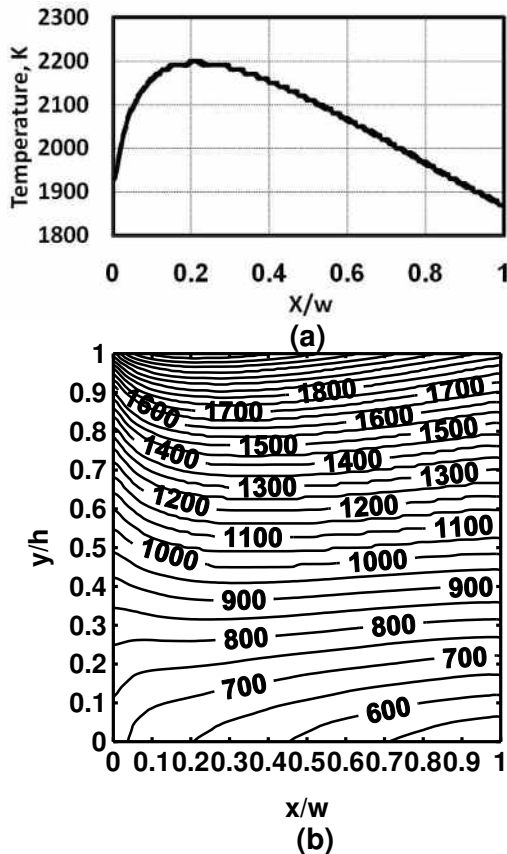


Fig. 4 Temperature variations, in Kelvin, through  $ZrO_2/6061-T6/Ti-6Al-4V$  2D-FGM plate for  $m_x=0.1$  and  $m_y=0.1$  where the maximum value of temperature is 2200 K.

(a) Through upper surface of the plate. (b) Through the whole of the plate.

Figure 5 shows the temperature variations, in Kelvin, through  $ZrO_2/6061-T6/Ti-6Al-4V$  2D-FGM plate for  $m_x=10$  and  $m_y=10$  where the maximum temperature value is 950 K. The nonhomogenous parameters,  $m_x=10$  and  $m_y=10$ , represent the case of 2D-FGM plate with aluminum alloy, 6061-T6, rich. This represents the best case of material composition since minimum value of the maximum temperature was achieved. Also, it can be noticed that the maximum temperature was achieved on the upper ceramic surface. In addition, such composition reduces the maximum induced temperature by 57% compared with using of material composition with the

nonhomogenous parameters  $m_x = 0.1$  and  $m_y = 0.1$ . Therefore such case should be adopted because of achieving minimum value of maximum temperature in spite of the maximum temperature was induced on the ceramic surface. Since the coefficient of thermal expansion is variable through the adopted plates therefore optimization process through thermal stresses should be carried out.

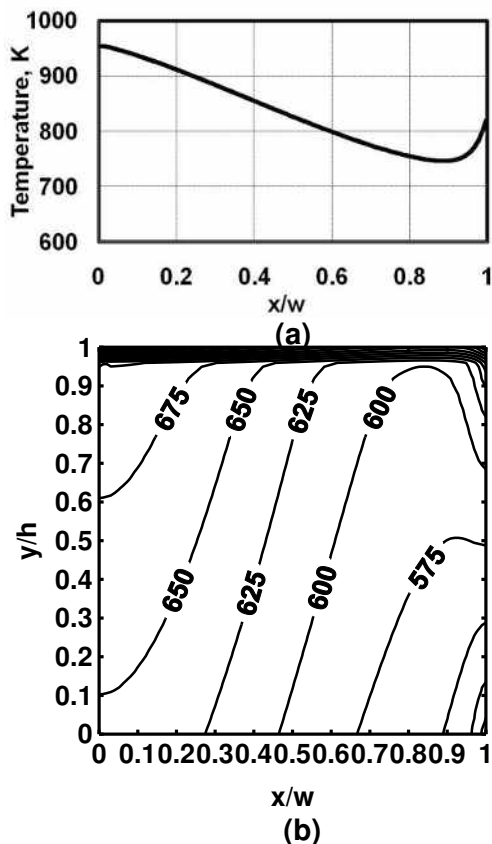


Fig. 5 Temperature variations, in Kelvin, through  $ZrO_2/6061-T6/Ti-6Al-4V$  2D-FGM plate for  $m_x = 10$  and  $m_y = 10$  where the maximum value of temperature is 950 K.  
 (a) Through upper surface of the plate. (b) Through the whole of the plate.

### 6-2- Reduction of Thermal Stresses

Figure 6 shows the variations of the maximum normalized equivalent stresses that resulted in the adopted  $ZrO_2/6061-T6/Ti-6Al-4V$  2D-FGM plates versus the values of the nonhomogenous parameters  $m_x$  and  $m_y$  during heating stage, where the maximum and minimum values are 2.0 and 0.8 respectively. It is clear that maximum value of the maximum normalized equivalent stresses was achieved for values of  $m_x$  and  $m_y$  of about 3 and 10 respectively. From equations (1) to (3) it can be concluded that this plate is aluminum alloy, 6061-T6, rich or ceramic,  $ZrO_2$ , poor while the volume fractions of Ti-6Al-4V is intermediate. Also, the minimum value of the maximum normalized equivalent stresses, 0.8, was achieved for values of  $m_x$  and  $m_y$  of about 0.1 and 5 respectively. From equations (1) to (3) it can be concluded that this plate is Ti-

6Al-4V alloy or ceramic,  $ZrO_2$ , poor while the volume fractions of 6061-T6 is intermediate.

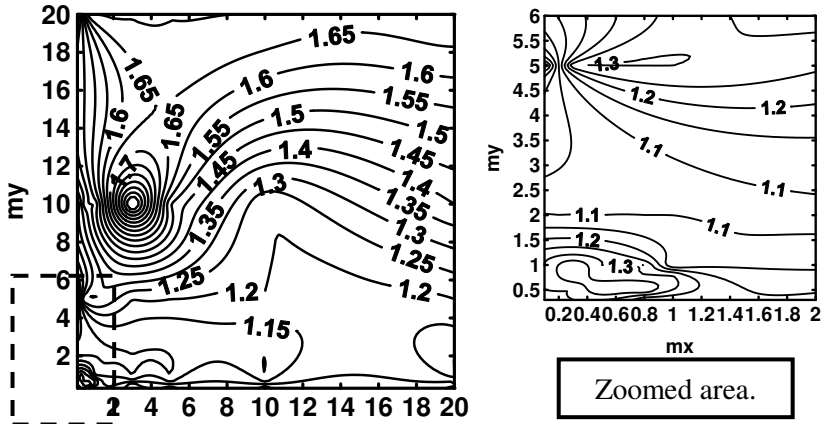


Fig. 6 Variations of the maximum normalized equivalent stresses that resulted in  $ZrO_2/6061-T6/Ti-6Al-4V$  2D-FGM plates versus the values of the nonhomogenous parameters  $m_x$  and  $m_y$  during heating stage where the maximum and minimum values are 2.0 and 0.8 respectively.

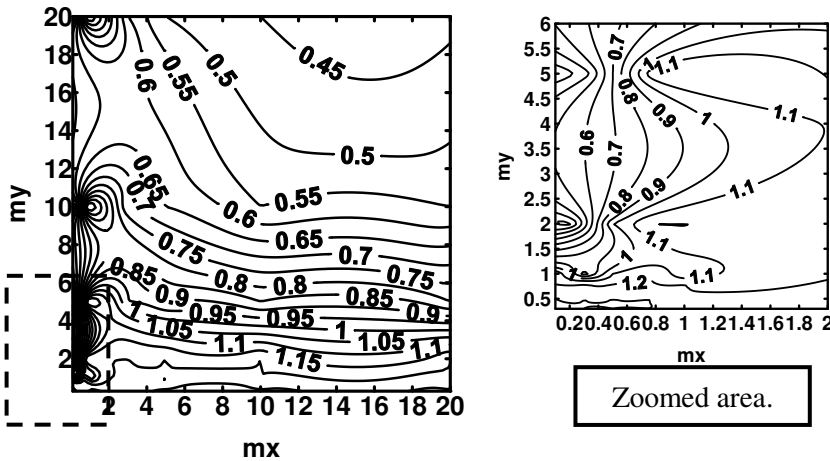


Fig. 7 Variations of the maximum normalized equivalent stresses that resulted in  $ZrO_2/6061-T6/Ti-6Al-4V$  2D-FGM plates versus the values of the nonhomogenous parameters  $m_x$  and  $m_y$  during cooling stage where the maximum and minimum values are 1.3 and 0.24 respectively.

Figure 7 shows the variations of the maximum normalized equivalent stresses that resulted in the adopted  $ZrO_2/6061-T6/Ti-6Al-4V$  2D-FGM plates versus the values of the nonhomogenous parameters  $m_x$  and  $m_y$  during cooling stage, where the maximum and minimum values are 1.3 and 0.24 respectively. It is clear that maximum value of the maximum normalized equivalent stress was achieved for values of  $m_x$  and  $m_y$  of about 7 and 0.2 respectively. From equations (1) to (3) it can be concluded that this plate is ceramic,  $ZrO_2$ , or Ti-6Al-4V alloy, poor while the volume fractions of 6061-T6 is intermediate.

Also, the minimum value of the maximum normalized equivalent stress, 0.24, was achieved for values of  $m_x$  and  $m_y$  of about 0.1 and 5 respectively. From equations (1) to (3) it can be concluded that this plate is Ti-6Al-4V alloy rich or ceramic,  $ZrO_2$ , poor while the volume fractions of 6061-T6 is intermediate.

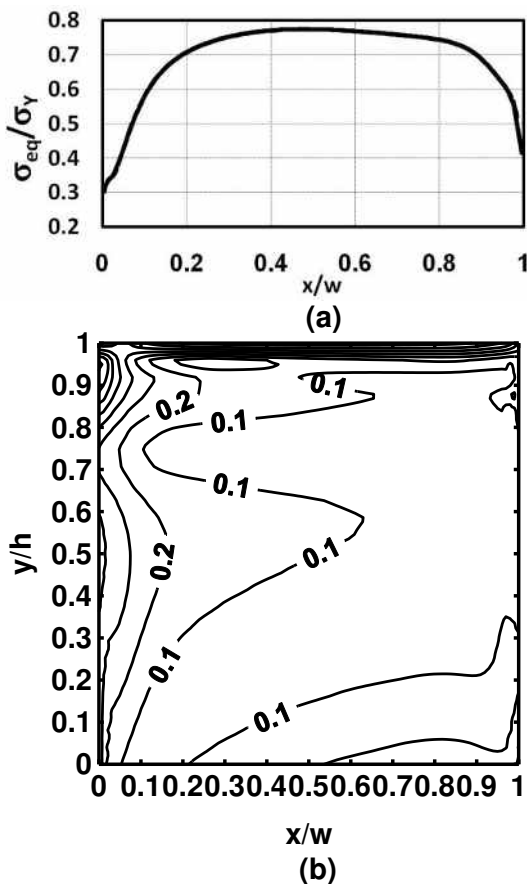


Fig. 8 Variation of the maximum normalized von Mises equivalent stresses  $\sigma_{eq}/\sigma_Y$ , for the optimum case ( $m_x = 0.1$  and  $m_y = 5$ ) during heating stage that was achieved at steady state where the maximum value is 0.8. (a) Through upper surface of the plate. (b) Through the whole of the plate.

Finally from Figs.6 and 7 it can be noticed that minimum values of maximum normalized equivalent stresses that are achieved in the adopted  $ZrO_2/6061-T6/Ti-6Al-4V$  2D-FGM plates during heating and cooling stages are elastic values which are 0.8 and 0.24 respectively. These values are induced in the same plate that has values of  $m_x$  and  $m_y$  of about 0.1 and 5 respectively. Also, from Figs. 6 and 7 it can be noticed that maximum values of maximum normalized equivalent stresses that are achieved in the adopted  $ZrO_2/6061-T6/Ti-6Al-4V$  2D-FGM plates during heating and cooling stages are 2.0 and 1.3 respectively. These values are inelastic values and represent the worst case of the induced thermal stresses during heating and cooling stages. This occurred for values of  $m_x$  and  $m_y$  of 3.0 and 10 for heating stage and 7 and 0.2 for cooling stage

respectively. These values are induced for different values of  $m_x$  and  $m_y$  which mean that they are induced in different plates.

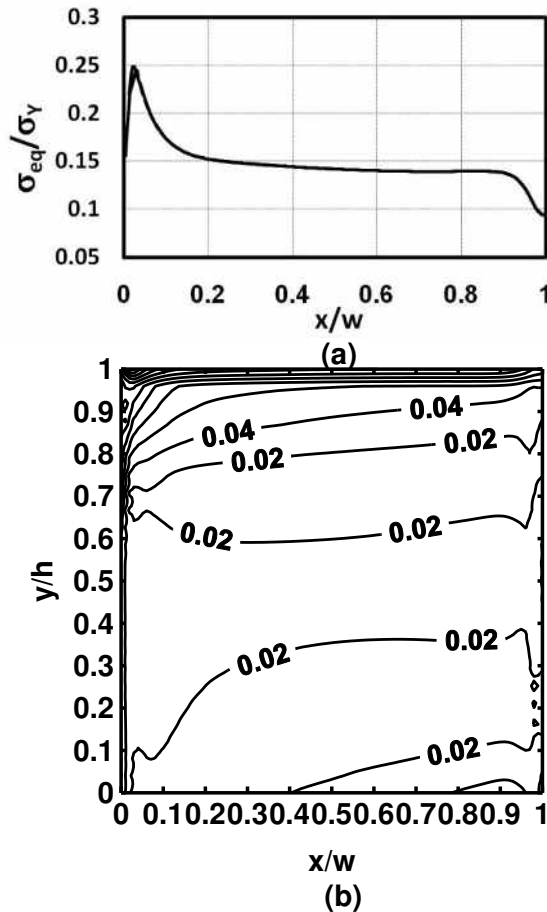


Fig. 9 Variation of the maximum normalized von Mises equivalent stresses  $\sigma_{eq}/\sigma_Y$ , for the optimum case ( $m_x = 0.1$  and  $m_y = 5$ ) during cooling stage that was achieved after starting of cooling process where the maximum value is about 0.24.

(a) Through upper surface of the plate. (b) Through the whole of the plate.

Figures 8 and 9 show the variation of the maximum normalized von Mises equivalent stresses  $\sigma_{eq}/\sigma_Y$ , for optimum case,  $m_x = 0.1$  and  $m_y = 5$ , during heating and cooling stages respectively. The maximum values are 0.8 and 0.24 for heating and cooling stages respectively and they are induced on the upper ceramic surface. These values are elastic values and hence the residual stresses should be zero in this plate under the adopted thermal loading cycle which is an important achievement. From the calculated values of the normalized equivalent residual stresses for the obtained optimum composition of ZrO<sub>2</sub>/6061-T6/Ti-6Al-4V 2D-FGM,  $m_x = 0.1$  and  $m_y = 5$ , it was found that the maximum value of the normalized equivalent residual stresses 0.035. This represents 3.5% from the yield stress which may be considered as an acceptable value of the numerical error and gives a confidence in the numerical results.

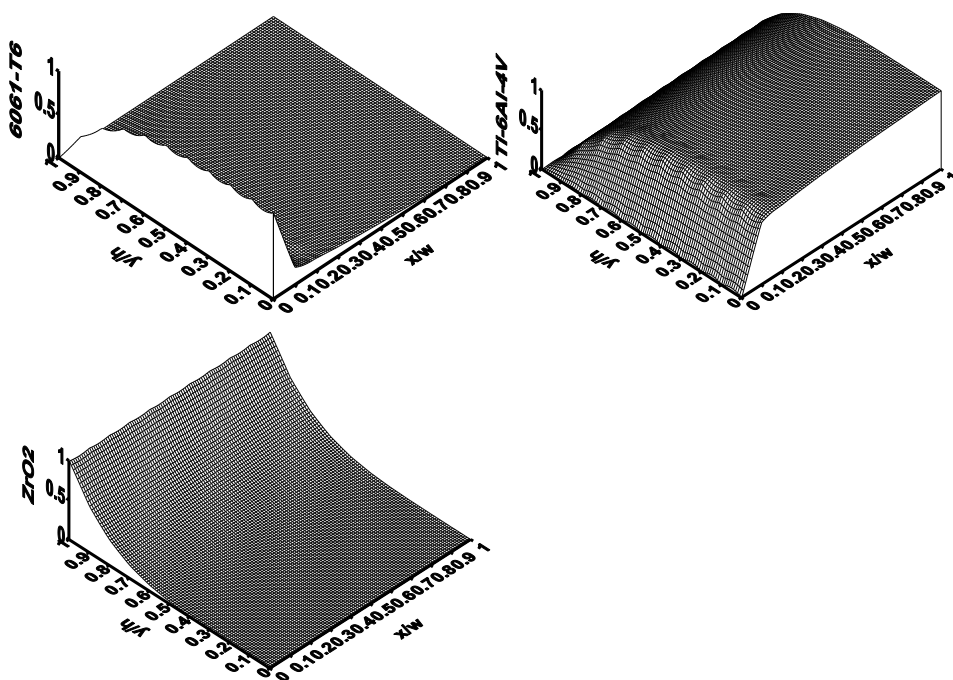


Fig. 10 Variations of the optimum composition of the three basic constituents of  $ZrO_2/6061-T6/Ti-6Al-4V$  2D-FGM, for  $m_x = 0.1$  and  $m_y = 5$ .

Figure 10 shows the optimum composition variations of the three basic constituents of  $ZrO_2/6061-T6/Ti-6Al-4V$  2D-FGM, with  $m_x = 0.1$  and  $m_y = 5$ . It is clear that the optimum composition is ceramic poor or metallic rich. It is noteworthy that the  $ZrO_2/6061-T6/Ti-6Al-4V$  2D-FGM, with  $m_x = 0.1$  and  $m_y = 5$ , metallic composition rich is Ti-6Al-4V rich or 6061-T6 poor. This may be attributed to the high strength of Ti-6Al-4V and high heat conductivity of 6061-T6 aluminum alloy.

## 7. CONCLUSIONS

Composition optimization of  $ZrO_2/6061-T6/Ti-6Al-4V$  2D-FGM, under prescribed severe thermal loading cycle was carried out. An elastic-plastic finite element model, adopting elastic-plastic strain hardening behavior, was used. From the results of the current investigation the following conclusions can be drawn;

- 1- Optimum composition based on the minimization of the induced temperature for  $ZrO_2/6061-T6/Ti-6Al-4V$  2D-FGM is achieved for  $m_x = 0.1$  and  $m_y = 0.1$ . While optimum composition based on minimization of the maximum normalized equivalent stresses for  $ZrO_2/6061-T6/Ti-6Al-4V$  2D-FGM is achieved for  $m_x = 0.1$  and  $m_y = 5$ .
- 2- Optimum composition of  $ZrO_2/6061-T6/Ti-6Al-4V$  2D-FGM that can withstand the adopted severe thermal loading is achieved for  $m_x = 0.1$  and  $m_y = 5$ .

- 3- The obtained optimum composition of ZrO<sub>2</sub>/6061-T6/Ti-6Al-4V 2D-FGM can stand well with the adopted severe thermal loading without any plastic deformation or residual stresses where the maximum value of the normalized equivalent stresses during heating stage is 0.8 and the maximum value of the normalized equivalent stresses during cooling stage is 0.24.
- 4- The optimum composition of ZrO<sub>2</sub>/6061-T6/Ti-6Al-4V 2D-FGM is ceramic, ZrO<sub>2</sub>, poor or metallic rich. Where metallic composition rich is Ti-6Al-4V rich or 6061-T6 poor.

## REFERENCES

- [1] Noda, N. and Tsuji, T., Steady thermal stresses in a plate of functionally gradient material, In FGM Forum Proc. 1<sup>st</sup> Int. Sym. on Functionally Gradient Materials, Sendai, Japan, pp.339-344, 1991.
- [2] Arai, Y., Kobayashi, K. and Tamura, M., Elastic-plastic thermal stresses analysis for optimum design of FGM, In FGM Forum Proc. Fourth National Sym. on Functionally Gradient Materials (FGM'91), Kawasaki, Japan, pp. 19-30, 1991.
- [3] Tang, X. F., Zhang, L. M., Zhang, Q. J. and Yuan, R. Z., Design and structural control of PSZ-MO functionally gradient materials with thermal Relaxation, In I.B. Holt et al (eds.), *Ceramic Transactions: Functionally Gradient Materials*, American Ceramic Society, Westerville, OH, **34**, pp. 45-463, 1993.
- [4] Noda, N., Thermal stresses intensity factor for functionally gradient plate with an edge crack, *J. Thermal Stresses*, Vol. 20, pp. 373-387, 1997.
- [5] Noda, N., Nakai, S. and Tsuji, T., Thermal stresses in functionally graded material of particle-reinforce composite, *JSME, series A*, Vol. 41, No. 2, pp.178-184, 1998.
- [6] Choules, B.D. and Kokini, K., Architecture of functionally graded ceramic coating against surface thermal fracture, *ASME J. Engineering Materials and Technology*, Vol. 118, pp 522-528, 1996.
- [7] Noda, N., Thermal stresses in functionally graded materials, *J. Thermal Stresses*, Vol. 22, pp. 477-512, 1999.
- [8] Steinberg, Morris A., *Materials for Aerospace*, U.S. goals for subsonic, supersonic and hypersonic flight and for space exploration call for alloys and composites notable for strength, light weight and resistance to heat, *Scientific American*, Vol. 244, pp. 59-64, 1986.
- [9] Callister, W, D. JR. *Materials science and engineering an introduction*, John Wiley, chapter 20, pp s347-s351, 2001.
- [10] Columbia Accident Investigation Board (2003). "Report of Columbia Accident Investigation Board, Volume I". NASA, January, 2006.
- [11] Columbia Accident Investigation Board (2003). "In-Flight Options Assessment, Volume II, appendix D.12 (PDF)". NASA, January, 2006.
- [12] Clements, D. L., Kusuma, J. and Ang, W. T., A Note on Antiplane Deformations of Inhomogeneous Materials, *Int. J. Engng. Sci.*, Vol. 35, pp.593-601, 1997.

- [13] Dhaliwal, R. S. and Singh, B. M., On the theory of elasticity of a non-homogeneous medium, *J. Elasticity*, Vol. 8, pp. 211-219, 1978.
- [14] Nemat-Alla, M. and Noda, N., Thermal stress intensity factor for functionally gradient half space with an edge Crack under thermal load, *Archive of Applied Mechanics*, Vol. 66 No.8, pp.569-580, 1996.
- [15] Nemat-Alla, M. and Noda, N., Study of an edge crack problem in a semi-infinite functionally graded medium with two dimensionally non-homogenous coefficient of thermal expansion under thermal load, *J. Thermal Stresses*, Vol.19, pp.863-888, 1996.
- [16] Nemat-Alla, M. and Noda, N., Edge crack problem in a semi-infinite FGM plate with a bi-directional coefficient of thermal expansion under two-dimensional thermal loading, *Acta Mechanica*, Vol.144, No. 2-3, pp. 211-229, 2000.
- [17] Nemat-Alla, M. and Noda, N. and Hassab-Allah, I., Analysis and investigation of thermal stress intensity factor for edge cracked FGM plates, *Bulletin of the Faculty of Engineering, Assiut university*, Vol. 29 Part 3(1/2), pp. 89-102, September, 2001.
- [18] Marin, M., Numerical solution of the Cauchy problem for steady-state heat transfer in two-dimensional functionally graded materials, *International Journal of Solids and Structure*, Vol.42, pp. 4338–4351, 2005.
- [19] Ke, L. L. and Wang, Y. S., Two-dimensional contact mechanics of functionally graded materials with arbitrary spatial variations of material properties, *International Journal of Solids and Structures*, Vol. 43, pp. 5779-5798, 2006.
- [20] Aboudi, J., Pindera, M. and Arnold, S., Thermoelastic theory for the response of materials functionally graded in two directions, *Int. J. Solids Structures*, Vol.33, pp.931-966, 1996.
- [21] Aboudi, J., Pindera, M. and Arnold, S., Thermoplasticity theory for bi-directionally functionally graded materials. *J. Thermal stresses*, Vol. 19, pp.809-861, 1996.
- [22] Cho, J.R. and Ha, D.Y., Optimal tailoring of 2D volume-fraction distributions for heat-resisting functionally graded materials using FDM, *Comput. Methods Appl. Mech. Engrg.*, 191, pp. 3195-3211, 2002.
- [23] Goupee, A. J. and Vel, S. S., Two-dimensional optimization of material composition of functionally graded materials using meshless analyses and a genetic algorithm, *Computer Methods in Applied Mechanics and Engineering*, Vol. 195, pp. 5926-5948, 2006.
- [24] Nemat-Alla, M., Reduction of thermal stresses by developing two-dimensional functionally graded materials, *International journal of solids and structures*, Vol.40, pp.7339-7356, 2003.
- [25] Wang, J., and Shaw, L. L., "Fabrication of Functionally Graded Materials Via Inkjet Color Printing", *J. Am. Ceram. Soc.*, Vol. 89, No. 10, pp. 3285–3289, 2006.
- [26] Nemat-Alla, M., Ahmed, K., and Hassab-Allah, I. "Elastic-Plastic Investigation on Effectiveness of Two Dimensional Functionally Graded Materials in Reduction of Thermal Stresses", *Journal of Engineering Sciences, Assiut University*, Vol. 36, No.3, pp. 689-710, 2008.

- [27] Tanigawa, Y., Oka, N., Akai, T. and Kawamura, R., One-Dimensional Transient Thermal Stress Problem for Nonhomogeneous Hollow Circular Cylinder and Its Optimization of Material Composition for Thermal Stress Relaxation, *JASME , Series A*, Vol. 40, pp.117-127, 1997.
- [28] Guo, Y.B., Wen, Q. and Horstemeyer, M.F., An internal state variable plasticity-based approach to determine dynamic loading history effects on material property in manufacturing processes, *International Journal of Mechanical Sciences*, Vol. 47, pp. 1423–1441, 2005.
- [29] Pettermann, H.E., Weissenbek, E. and Suresh, S., Simulation of Elsto-Plastic Deformations in Functionally Graded Metal-Ceramic Structure: Mean Field and Unit Cell Approaches, *FGM 96*, Shiota and Miyamoto, Editors, Elsevier Science B. V. pp., 75-80, 1997.
- [30] Suresh, S and Mortensen, A., Functionally Graded Materials and Metal-Ceramic Composites: Part-2 Thermomechanical Behaviour, *International Materials Review* Vol. 42, pp. 85-116, 1997.
- [31] Giannakopoulos, A. E., Suresh, S. Finot, M. and Olsson, M., Elstoplastic Analysis of Thermal Cycling Layered Materials with Compositional Gradients, *Acta Metall.* Vol. 43, pp. 1335-1354, 1995.
- [32] Aboudi, A., Pindera, M. J. and Arnold, S. M., Thermo-Inelastic Response of Functionally Graded Composites, *International journal of solids and structures*, Vol.32, pp.1675-1710, 1995.
- [33] Tohgo, K., Masunari, A. and Yoshida, M., Two-phase composite model taking into account the matrixity of microstructure and its application to functionally graded materials, *Composites: Part A*(In press), Vol. pp. , 2006.
- [34] Jin, Z.-H., Effect of material nonhomogeneities on the HRR dominance, *Mechanics Research Communications*, Vol. 31, pp.203–211, 2004.
- [35] Gu, Y., Nakamura, T., Prchlik, L., Sampath, S. and Wallace, J., Micro-indentation and inverse analysis to characterize elastic-/plastic graded materials, *Materials Science and Engineering-A* Vol.345, pp. 223-/233, 2003.
- [36] Aboudi, A., Pindera, M. J. and Arnold, S. M., Higher-order theory for periodic multiphase materials with inelastic phases, *International Journal of Plasticity*, Vol. 19, pp.805–847, 2003.
- [37] Shim, D. J., Paulino, G. H. and Jr, R. H. D., A Boundary Layer Framework Considering Material Gradation Effects, *Engineering Fracture Mechanics*, Vol. 73, pp.593-615, 2006.
- [38] Jin, Z.H. and Jr, R. H. D., Crack growth resistance behavior of a functionally graded material: computational studies, *Engineering Fracture Mechanics*, Vol. 71, pp. 1651–1672, 2004.
- [39] Jin, Z.H., Paulino, G. H. and Jr, R. H. D., Cohesive fracture modeling of elastic-plastic crack growth in functionally graded materials, *Engineering Fracture Mechanics*, Vol. 70, pp. 1885–1912, 2003.
- [40] Tvergaard, V., Theoretical investigation of the effect of plasticity on crack growth along a functionally graded region between dissimilar elastic–plastic solids, *Engineering Fracture Mechanics*, Vol. 69, pp. 1635–1645, 2002.

- [41] Kokini, K. and Case, M., Initiation of surface edge cracks in functionally graded ceramic thermal barrier coating, ASME journal of Materials and technology, Vol. 119, pp. 148-152, 1997.
- [42] Li C, Zou Z, Duan Z. Multiple isoparametric finite element method for nonhomogeneous media, Mech Res Commun, vol. 27(2), pp.137–142, 2000.
- [43] Bleek O, Munz D, Schaller W, Yang YY., Effect of a graded interlayer on the stress intensity factor of cracks in a joint under thermal loading, Engng. Fract. Mech., vol.60, No. (5–6), pp.615–623, 1998.
- [44] Bao G, Wang L. Multiple cracking in functionally graded ceramic/metal coatings, Int. J Solid Struct., vol. 32, No.(19), pp.2853–2871, 1995.
- [45] Li, H., Lambros J, Cheeseman BA, Santare MH., Experimental investigation of the quasi-static fracture of functionally graded materials, Int. J Solid Struct., vol.37, pp.3715–3732, 2000.
- [46] Santare MH, Lambros J., Use of graded finite elements to model the behaviour of nonhomogeneous materials, J App. Mech., vol. 67, pp. 819–822, 2000.
- [47] Kim J-H, Paulino GH., Isoparametric graded finite elements for nonhomogeneous isotropic and orthotropic materials, ASME J Appl. Mech., vol. No. 69, pp.502–514, 2002.
- [48] Rousseau CE, Tippur HV., Compositionally graded materials with cracks normal to the elastic gradient, Acta Mater., vol. 48, pp. 4021–4033, 2000.
- [49] Nemat-Alla, M. Ahmed, K.I., 3-D elastic-plastic finite element analysis of two dimensional functionally graded materials under cyclic thermal loading, 7<sup>th</sup> international congress on thermal stresses, June 4-7, Taipei, pp 321-324, 2007.

### التركيب الأمثل للمواد المُدرّجة وظيفيا ثنائية الأبعاد تحت تأثير الاحمال الحرارية

إن تخفيض الإجهادات الحرارية في عناصر الماكينات التي تتعرض إلى احمال حرارية عالية امكن تحقيقه عن طريق استخدام المواد المُدرّجة وظيفيا ثنائية الأبعاد *2D-FGM*. في هذا البحث تم الحصول على التركيب الأمثل لالوح من المواد المُدرّجة وظيفيا ثنائية الأبعاد *ZrO<sub>2</sub>/6061-T6/ TI-6AL-4V* تحت تاثير دورة من التحميل الحراري الحادّ المكون من عملية تسخين تليها عملية تبريد، عن طريق تقليل قيم درجات الحرارة والإجهادات الحرارية و المتبقية المتولدة في اللوح. وقد وجد ان التركيب الأمثل بناء على قيم درجات الحرارة القصوى المتولدة في اللوح يمكن تحقيقه عند القيم التالية لمعاملات عدم التجانس في الاتجاه السيني والصادي  $m_x = 0.1$  and  $m_y = 0.1$ . بينما وجد ان التركيب الأمثل بناء على قيم الإجهادات الحرارية القصوى المتولدة في اللوح يمكن تحقيقه عند القيم

التالية لمعاملات عدم التجانس فى اتجاه السينى والصادى  $m_x = 0.1$  and  $m_y = 5$ . وان التركيب الامثل للالواح من المواد المُدرَّجَة وظيفيا ثنائية الأبعاد يُمكن أن يقاوم التحميل الحرارى الحادّ المُتَبَنَّى بدون أيّ تشوه لدن أو إجهادات متبقية وان أقصى قيمة للإجهادات المكافئة أثناء مرحلة التسخين هو 0.8 من قيمة اجهاد الخضوع و أثناء مرحلة التبريد هو 0.24 من قيمة اجهاد الخضوع.